We are IntechOpen,
the world's leading publisher of
Open Access books
Built by scientists, for scientists

4,800
Open access books available

122,000
International authors and editors

135M
Downloads

Our authors are among the

154
Countries delivered to

TOP 1%
most cited scientists

12.2%
Contributors from top 500 universities

CLARIVATE ANALYTICS

BOOK
CITATION
INDEX

INDEXED

WEB OF SCIENCE™

Selection of our books indexed in the Book Citation Index
in Web of Science™ Core Collection (BKCI)

Interested in publishing with us?
Contact book.department@intechopen.com

Numbers displayed above are based on latest data collected.
For more information visit www.intechopen.com

Chapter

The Viscosity Behaviour of PEGylated Locust Bean Gum/Rosin Ester Polymeric Nanoparticles

Selcan Karakus, Merve Ilgar, Ezgi Tan, Yeşim Müge Sahin, Nevin Tasaltin and Ayben Kilislioglu

Abstract

In this study, PEGylated locust bean gum–rosin glycerol ester polymeric nanoparticles (PEG-LBG/RE PNPs) were synthesized by using simple ultrasonic irradiation method. The nanoparticles were characterized by using Fourier-transform infrared spectroscopy (FTIR) and scanning transmission electron microscopy (STEM). The viscosity behaviors of nanoparticles were studied in different conditions (pH, sonication time, and salt). The experimental results were calculated by Huggins, Kraemer, Tanglertpaibul-Rao, and Higiro models to understand the colloidal stability, the miscibility mechanism, and coefficients of nanoparticles. The results confirmed that the homogenous distribution of nanostructure was related to sonication time (30 min) and the presence of NaOH salt. With the addition of NaOH, the nanosystem based on ionotropic gelation technique was made more homogeneous. The results made us think that nanoparticles can be a good candidate for drug delivery systems in biomedical and pharmaceutical applications.

Keywords: ultrasonic-assisted, locust bean gum, rosin glycerol ester, polymeric nanoparticles

1. Introduction

Colloidal nanoparticles (CNPs) have attracted attention in industrial applications (food, pharmaceuticals, cosmetics, ink, rubber, and water treatment) due to their biological, mechanical, and thermal properties and stability in solution. Their superior properties depend on the high surface area, small size, and uniform morphologies [1–3]. CNPs are prepared to use different methods such as sol–gel [4], photochemical [5], electrochemical [6], laser ablation [7], ionizing irradiations [8], and ultrasonic irradiation [9].

The ultrasonic irradiation synthesis of different morphologies of nanomaterials consisted of metal/metal oxides, and polymeric materials have received considerable attention in the nanotechnology applications. The ultrasonic irradiation (20 kHz to 10 MHz) method has been employed in the preparation of the high purity, the uniform shape, and the nanosized distribution of nanomaterials.

This method causes the formation of the acoustic cavitations which consist of the bubbles [10]. The growth and collapse of bubbles are related to the transfer of energy at high pressures and temperatures due to the highly reactive free radicals such as hydrogen radicals (H•) and hydroxyl radicals (OH•). Bubbles generate three zones, such as a hot spot (5000°C, 500 atm), a gas–liquid interface (300°C, 50 atm), and a bulk solution (25°C, 1 atm) [11].

In recent research, different structures of nanoparticles such as TiO_2 [12], ZnO [13], starch [14], alumina/carbon core-shell [15], lipid-polymer hybrid [16], and biopolymeric [17, 18] nanoparticles have been synthesized with the ultrasonic irradiation method. Generally, biopolymeric nanoparticles have used in the field of foods encapsulation and drug delivery studies due to the biodegradability, biocompatibility, and low toxicity properties. Alginate [19], chitosan [20], carboxymethyl cellulose/gelatin [21], Senegal gum [22], guar gum [23], xanthan gum [24], *Senna tora* gum [25], and locust bean gum (LBG) [26] are natural biopolymers employed in industrial processes [24]. Locust bean gum is a neutral polysaccharide and has a mannose backbone with single side chain galactose units [25–27].

When the studies in the current literature are examined, it has been found that there are very few studies on LGB based on nanoparticles [28–30]. It was found that no studies were performed on the locust nanostructures containing rosin gum and derivatives. In this work, the ultrasonic irradiation method was used for the preparation of novel PEGylated locust bean gum (PEG-LBG)/rosin glycerol ester (RE) polymeric nanoparticles (PNPs) at room temperature. The present research work was aimed at the colloidal stability, the viscosity behaviour, and miscibility of binary polymer blends of PEG and LBG PNPs due to the intrinsic viscosity. The intrinsic viscosity of the polymer is a significant molecular characteristic, depending on the size of the polymer chain, molecular weight, and radius of rotation of the polymer in dilute solution. The voluminosity (VE), shape factor (υ), the intrinsic viscosity [η], and Krigbaum and Wall miscibility parameter (Δb) of polymeric nanoparticles were calculated from different models such as Huggins, Kraemer, Tanglertpaibul-Rao, and Higiro [17]. The values of intrinsic viscosities were used to determine the rheological behaviour of the PEG-LBG/RE PNPs at different conditions (pH, sonication time, and salt). The homogeneous distributions of PEG with LGB had an influence on the blends ratio of PEG/LBG (1:1, 1:2), sonication time (10–70 min.), temperature (25–35°C), and salts (NaOH, KOH, CTAB). With the addition of NaOH salt, PEG-LBG/RE PNPs based on ionotropic gelation technique were made into a more homogeneous solution. The PEG-LBG/RE PNPs were characterized to examine surface morphologies using a Fourier-transform infrared spectroscopy (FTIR) and scanning transmission electron microscopy (STEM). The aim of this study was to provide an investigation of rosin ester-based nanoparticle distributions in LGB and understand the role of polymer–particle interactions with respect to nanoparticle concentration as well to use the candidate nanocarrier for biomedical applications.

2. Materials and methods

2.1 Materials

Locust bean gum from *Ceratonia siliqua* seeds (M.W. of approx. 310 kDa) was purchased from Sigma Aldrich. Polyethylene glycol (PEG 400) was obtained from Fluka (Switzerland). Ethyl acetate (anhydrous, 99.8%) was purchased from Sigma Aldrich. Dimethyl sulfoxide (DMSO), potassium hydroxide (KOH), sodium hydroxide (NaOH), and cetyltrimethylammonium bromide (CTAB) were

purchased from Merck. Rosin glycerol ester was purchased from Pina Kimya (CAS: 8050-26-8, EC: 232–479-9, Turkey). All other reagents and chemicals were of analytical grade.

2.2 Preparation of PEG-LBG/RE polymeric nanoparticles

PEG-LBG/RE PNPs were synthesized using the ultrasonic irradiation method (Ultrasonics Vibra-Cell, probe type, amplitude %30, a frequency of 20 kHz) with different ratios of blends (PEG-LBG: 1:1, 1:2). In the procedure, two phases were prepared such as the dispersion phase and the continuous phase.

The continuous phase: 125 mg LBG was dissolved in 50 ml of distilled water (60°C for 20 min) and then added to 125 mg of PEG400 polymer solution at room temperature.

The dispersion phase: 0.01 g RE was dissolved in 0.5 ml DMSO and then 7 ml ethyl acetate was added to the solution.

7.5 ml of continuous phase and the dispersed phase was sonicated at room temperature. 42.5 ml of continuous phase was then added slowly to the blends, and the sonication procedure was continued for 30 minutes. The final solution was evaporated at room temperature for 14 hours until ethyl acetate completely evaporated in the solution. Polymer blends were also performed for different composition ratios (PEG-LBG) such as 1:1 and 1:2.

2.3 Characterization parts

The dynamics viscosities of LBG, PEG-LBG, and PEG-LBG/RE were determined by a programmable AND viscometer (SV-10, Sine-wave Vibro Viscometer, A δ D Company). PEG-LBG/RE PNPs were scanned in the dark field area with the wet STEM detector by using FEI QUANTA S50 (A copper grid, Ted Pella, support films, carbon type A, 300 meshes was utilized). STEM holder was cooled to 2°C and the pressure was set between 700 and 1300 Pa. Samples were ground with KBr powder and analyzed from 4000 to 600 cm^{-1} with a resolution of 4 cm^{-1} using 8 scans by using a PerkinElmer FTIR emission spectrometer.

2.4 Calculations of the multi-concentration regression models

The changes in viscosity values of LBG, PEG-LBG, and PEG-LBG/RE PNPs were investigated in a dilute solution (50 mL) at different ratios of polymer blends (PEG-LBG: 1:1 and 1:2), temperatures (25 and 35°C), and sonication times (10–70 min) in

		Formula	Ref:
Specific viscosity	$\eta_{sp} = \frac{t}{t_0} - 1$	(1)	[31]
Intrinsic viscosity	$[\eta] = \lim_{C \to 0} \left(\frac{\eta_{sp}}{C} \right)$	(2)	[31]
	Multi-concentration regression models:		
Huggins	$\eta_{sp}/C = [\eta] + k_1[\eta]^2 C$ (k_1, Huggins constant)	(3)	[32]
Kraemer	$\ln \eta_{rel}/C = [\eta] + k_2[\eta]^2 C$ (k_2, Kraemer constant)	(4)	[33]
Tanglertpaibul-Rao	$\eta_{rel} = 1 + [\eta]C$	(5)	[34]
Higiro	$\eta_{rel} = e^{[\eta]C}$	(6)	[28]

Table 1.
The equations of the intrinsic viscosity, the specific viscosity, and the multi-concentration regression models.

the presence of NaOH, KOH, and CTAB salts. The specific viscosities (η_{sp}), the intrinsic viscosities ($[\eta]$), and the multi-concentration regression models of PEG-LBG/RE PNPs were calculated by using an AND viscometer (WinCT-Viscosity software) in 50 ml solution at constant temperature [31–36] (**Table 1**).

In this study, the voluminosity (VE), shape factor (υ), and Krigbaum and Wall parameter (Δb) were calculated using the following Eqs. 7–10, respectively. The polymer blends are miscible if $\Delta b \geq 0$ and immiscible when $\Delta b < 0$. (b_{12}^*, the experimental interaction parameter; b_{12}, the theoretical interaction parameter):

$$\gamma = \frac{\eta_{rel}^{0.5} - 1}{C\left(1.35\eta_{rel}^{0.5} - 0.1\right)} \tag{7}$$

$$[\eta] = \upsilon V_E \tag{8}$$

$$b_{12}^* = \sqrt{b_{11}b_{22}} \tag{9}$$

$$\Delta b = b_{12} - b_{12}^* \tag{10}$$

3. Results and discussions

3.1 Colloidal stability and viscosity analysis

3.1.1 The multi-concentration regression models and salt factor

The intrinsic viscosity of $[\eta]$ of PEG, LBG, PEG-LBG (1:1), and PEG-LBG/RE 1:1 nanoparticles was calculated using the multi-concentration regression models (Huggins, Kraemer, Tanglertpaibul-Rao, and Higiro models) at room temperatures. The correlation coefficient (R^2), the intrinsic viscosity, and parameters of Huggins,

		Huggins			Kraemer			Tanglertpaibul-Rao		Higiro	
	pH	$[\eta]$ (ml/g)	$k_1 \times 10^{-3}$	R^2	$[\eta]$ (ml/g)	k_2	R^2	$[\eta]$ (ml/g)	R^2	$[\eta]$ (ml/g)	R^2
A		4.70	0.213	0.99	6.73	1.129	0.89	9.11	0.96	10.87	0.98
B		5.18	0.193	0.99	56.75	−0.075	0.87	41.32	0.98	12.68	0.99
C		2.25	0.445	0.96	71.95	−0.067	0.86	41.57	1.00	12.65	0.99
D		0.67	1.493	0.99	55.78	−0.073	0.87	43.94	1.00	10.97	0.99

Samples: (A) PEG, (B) LBG, (C) PEG-LBG/ (1:1), (D) PEG-LBG/RE (1:2), and (E) PEG-LBG/RE (1:1).

Table 2.
The intrinsic viscosity (ml/g) values of PEG-LBG blends and PEG-LBG/RE nanoparticles at room temperature for different concentrations.

	V_E (ml/g)	υ		Δb (mL/g)^2	Miscibility
PEG-LBG (1:1)	38	2.5>	spherical	1.59	Miscible
PEG-LBG/RE PNPs (1:2)	42	—		−0.64	İmmiscible
PEG-LBG/RE PNPs (1:1)	35	2.5 >	spherical	1.56	Miscible

Table 3.
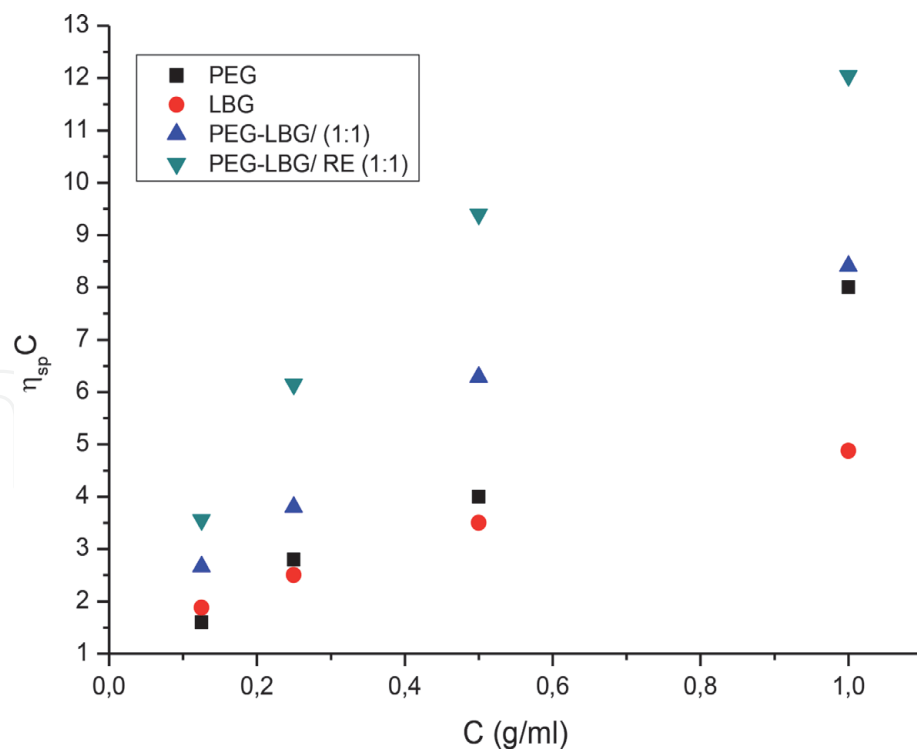*Voluminosity and shape factor of LBG, PEG-LBG, and PEG-LBG/RE PNPs.*

Figure 1.
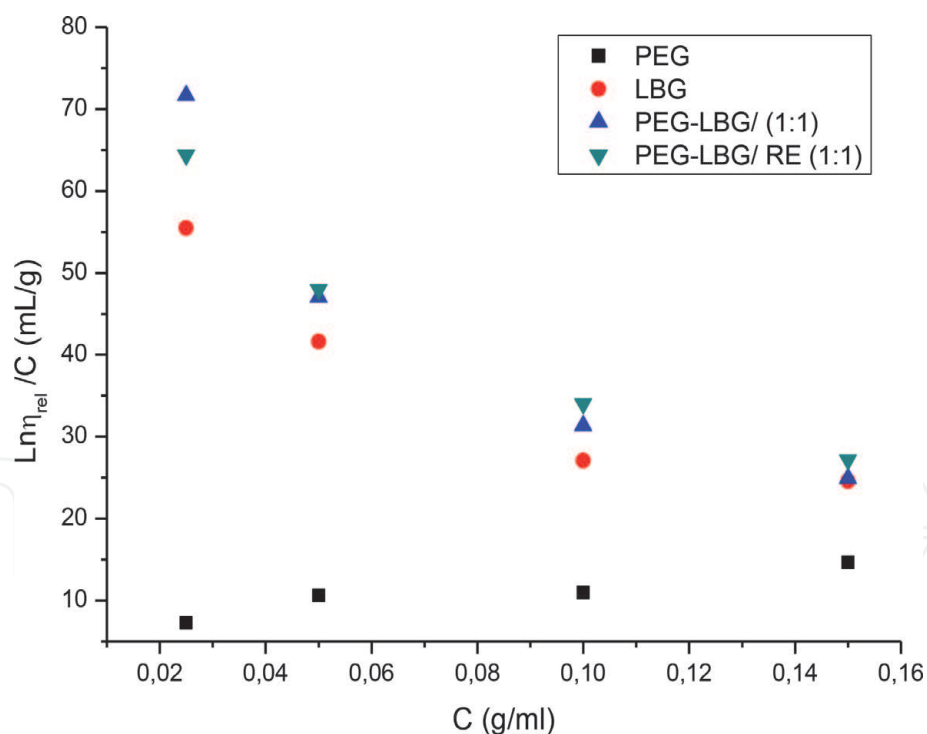*The Huggins plots of PEG, LBG, PEG-LBG (1:1), and PEG-LBG/RE PNPs.*

Figure 2.
The Kraemer plots of PEG, LBG, PEG-LBG (1:1), and PEG-LBG/RE PNPs.

Kraemer, Tanglertpaibul-Rao, and Higiro models were given comparatively in **Table 2** (**Figures 1–4**). In this study, we focused on the effect of nanoparticles on the morphology of immiscible polymer blends. We found that PEG-LBG/RE PNPs (1:2) were immiscible due to the mixing ratio of PEG-LBG (**Table 3**).

The Huggins, Kraemer, Tanglertpaibul-Rao, and Higiro plots of the intrinsic viscosities were calculated at different blend ratios, and the results showed the critical role on relation between the intrinsic viscosities and the blend ratios.
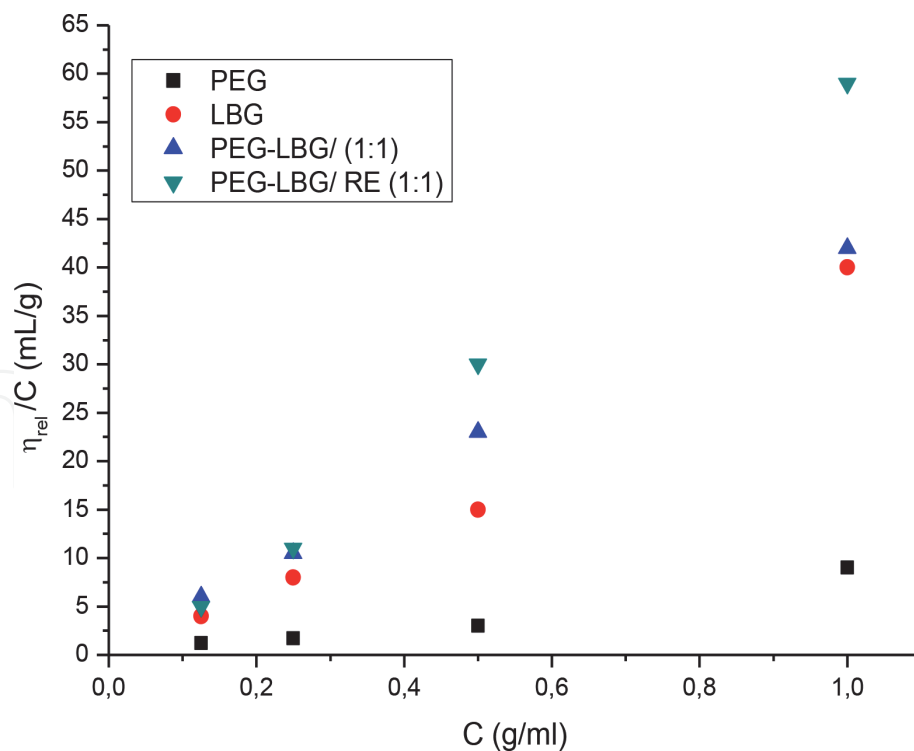
Figure 3.
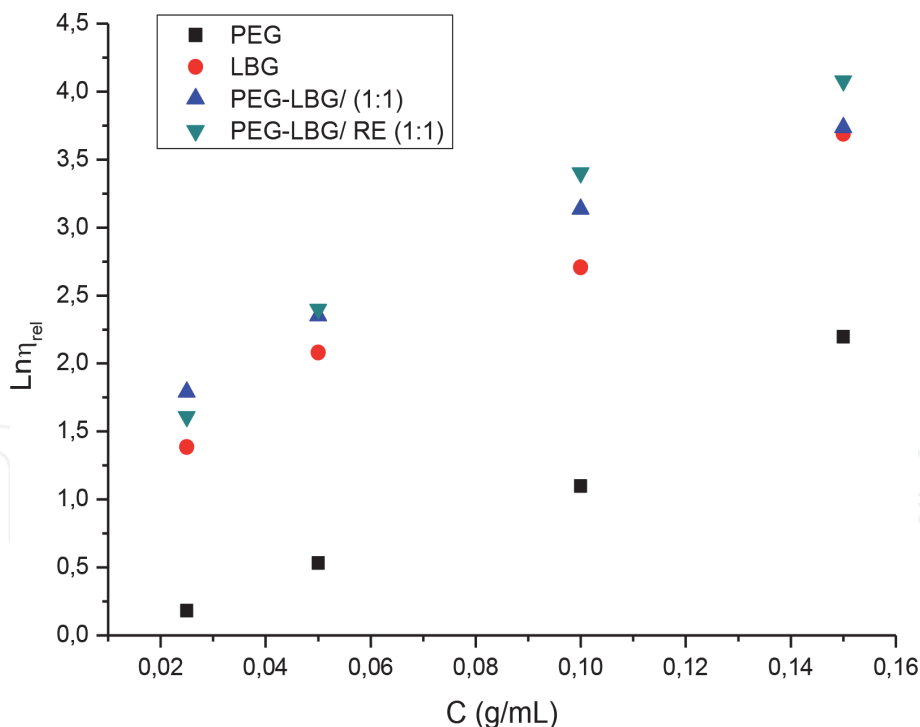*The Tanglertpaibul-Rao's plots of PEG, LBG, PEG-LBG (1:1), and PEG-LBG/RE PNPs.*

Figure 4.
The Higiro plots of PEG, LBG, PEG-LBG (1:1), and PEG-LBG/RE PNPs.

The Tanglertpaibul-Rao model and Huggins model (R^2 = 0.96–1.00) were the best models to understand the intrinsic viscosity of PEG, LBG, PEG-LBG, and PEG-LBG/RE PNPs. Behrouzian et al. [32] reported that the Tanglertpaibul and Rao model was the best model for the intrinsic viscosity determination of cress seed gum
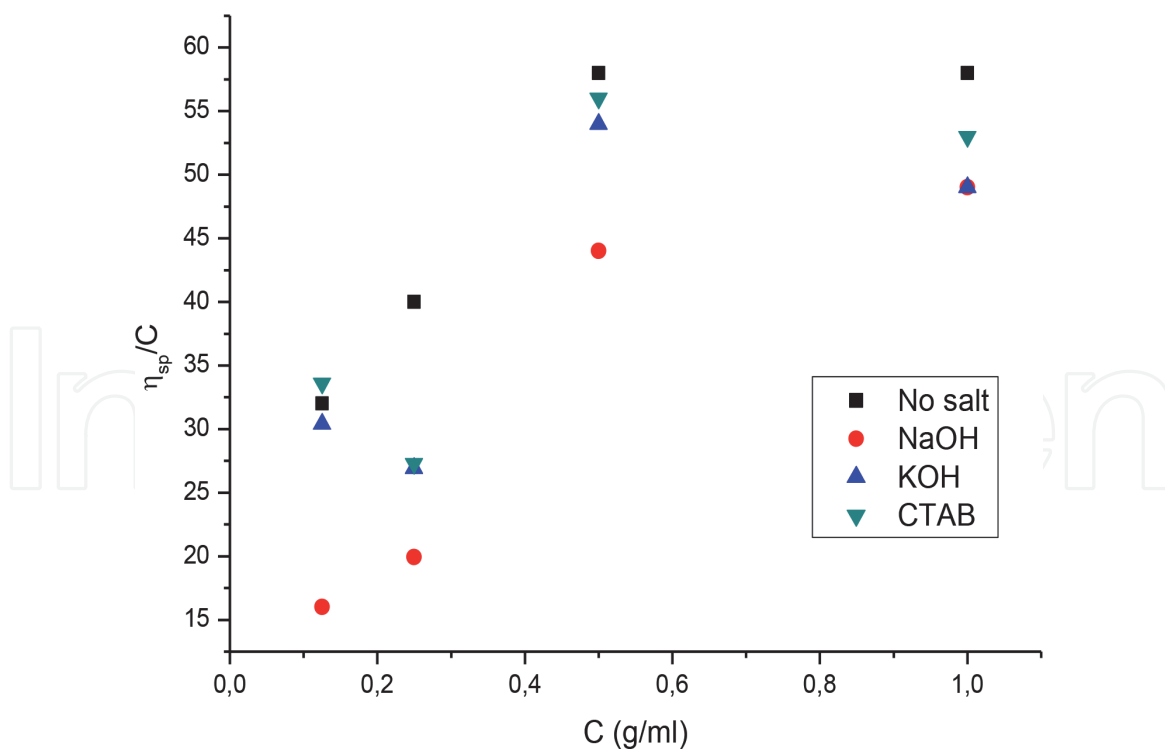
Figure 5.
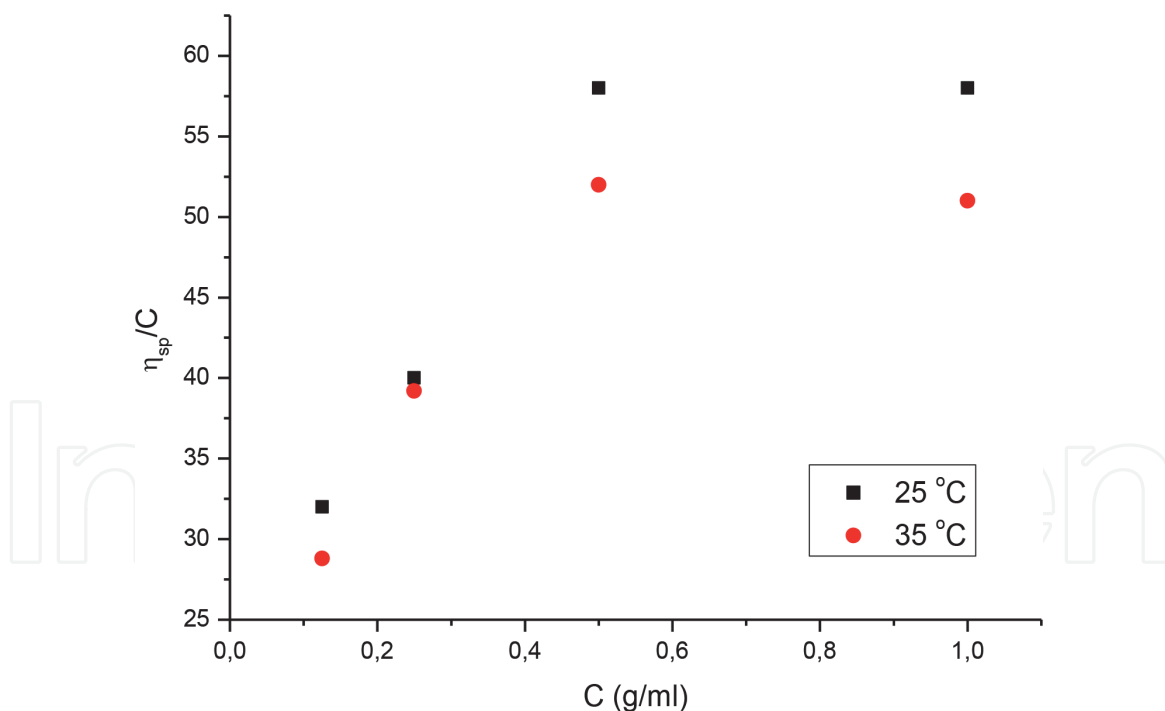*Plots of the intrinsic viscosity versus C of PEG-LBG/RE PNPs in the presence of salts (KOH, NaOH, and CTAB).*

Figure 6.
Plots of [η] of PEG-LBG/RE PNPs at different temperatures (25 and 35°C).

solutions. Razavi et al. [37] reported that the best model was Tanglertpaibul and Rao model for wild sage seed gum. In this study, the intrinsic viscosity of PEG-LBG/RE PNPs in the presence of different salts (NaOH, KOH, and CTAB) was investigated (Csalt, 0.1 M; Vsalt, 2 mL; Vsolution; 50 mL) at 25°C. The effect of NaOH, KOH, and CTAB salts on the values of intrinsic viscosity of PEG-LBG/RE PNPs (1:1) was presented in **Figure 5**.

The pH values of the solutions (LBG, PEG-LBG, and PEG-LBG/RE PNPs) at initial pH in KOH, NaOH, and CTAB salt additions were determined: $pH_{initial}$, 5.7; $pH_{initial}$, 5.55; and $pH_{initial}$, 5.32, respectively. In the presence of salt, the values of the intrinsic viscosity for the mixture were observed to change in two different salts such as KOH (pH_{final}: 5.93) and NaOH (pH_{final}: 5.72). The [η] values for PEG-LBG/RE PNPs (1:1) did not exhibit distinctive changes in the presence of CTAB (pH_{final}: 3.87). Jiang et al. [38] reported that the interactions between blends were dependent on the ionic strength at low salt concentration which was related to the increase of salt concentration. Consequently the addition of NaOH and KOH showed the electrostatic repulsion between charges along the backbone of the polymer blends.

3.1.2 Temperature and sonication time factor

The intrinsic viscosity decreased when the temperature increased, and the relation of the experimental results of PEG-LBG/RE PNPs with the temperature was shown in **Figure 6**.

However, when PEG-LBG/RE PNPs were sonicated, the intrinsic viscosity decreased for 30 minutes but remained constant after a period of time. These results had proven that the sonication time changed the value of viscosity and was effective on the blends (30% amp., 25°C) (**Figure 7**). The viscosity of Cu-ethylene glycol (EG) nanofluids was proven to decrease with the sonication time [39]. In this study, we found a similar situation, and demonstrated that sonication time changes the viscosity, which has a role on the formation of nanoparticles.

3.1.3 The voluminosity, shape factor, and miscibility parameter

In this study, we investigated the relationship between the intrinsic viscosity and the surface morphology, particle size, and shape. The shape factor was calculated using the approach given as follows: (a) n < 2.5 indicates spherical shape, and (b) n > 2.5 indicates ellipsoidal particles [40].
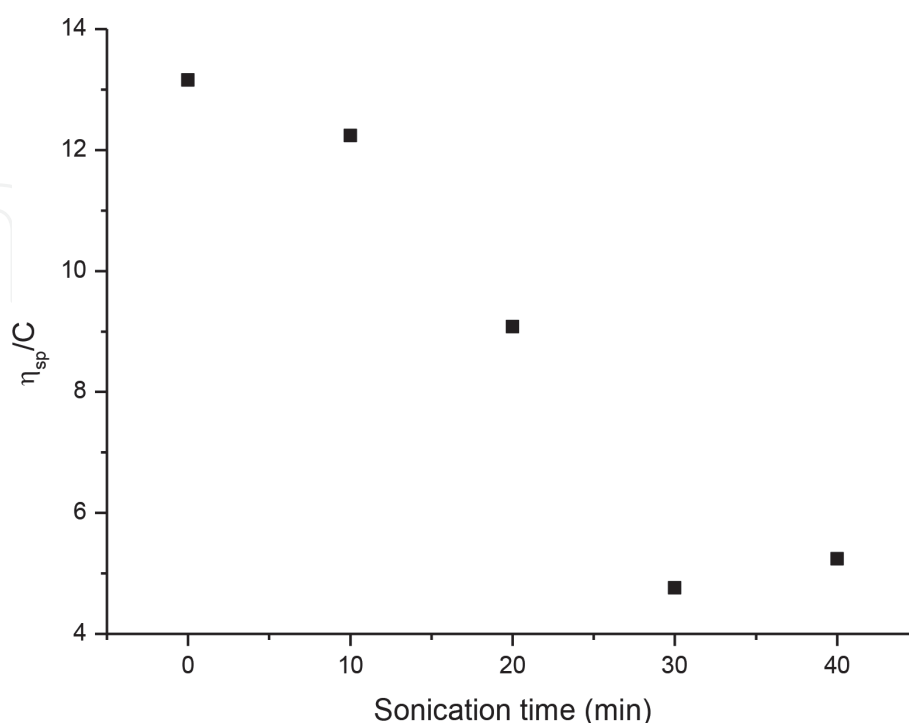

Figure 7.
Plots of [η] of PEG-LBG/RE PNPs at different sonication times (30% amp., 25°C).
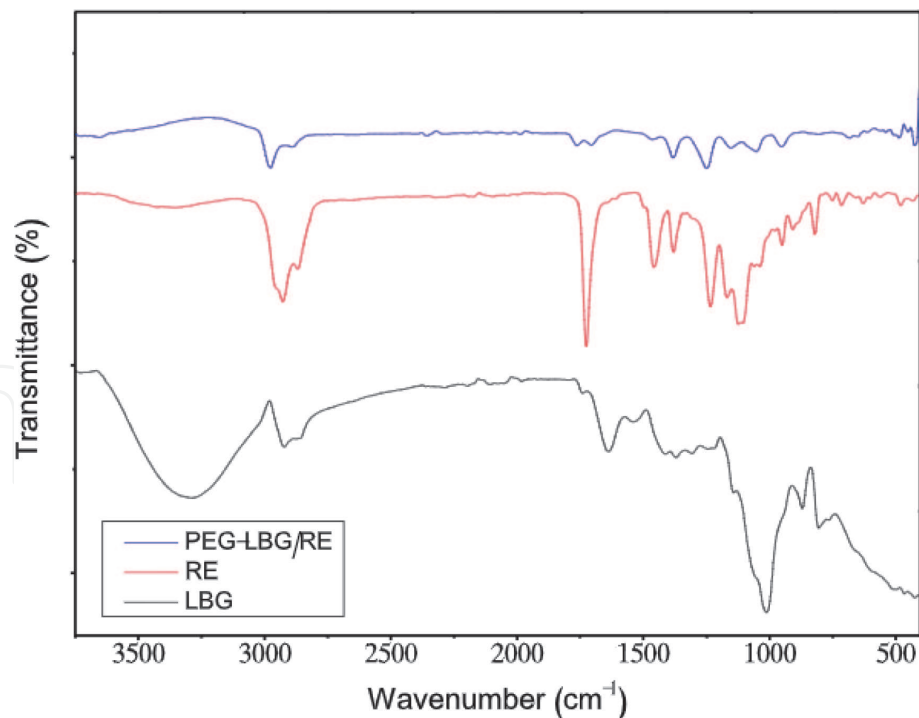
Figure 8.
The FTIR spectrum of pure LBG, pure RE, and PEG-LBG/RE PNPs.

In this study, we predicted the size and shape factor of PEG-LBG (1:1), PEG-LBG/RE PNPs (1:1), and PEG-LBG/RE PNPs (1:2) using the values of the intrinsic viscosity, associated with the shape factor, which were used to determine the change in the structure configuration. We calculated the shape and the Krigbaum and Wall (Δb) parameters of PEG-LBG/RE PNPs (1:1) using the intrinsic viscosity to determine the changes in the blends. We found that PEG-LBG/RE PNPs (1:1) had a spherical-like configuration, and the amounts of PEG had a role on the miscibility due to the interactions between the functional groups in the blends.

3.2 FTIR analysis

The FTIR spectra of pure LBG, pure RE, and PEG-LBG/RE PNPs were shown in **Figure 8**.

The FTIR spectrum of pure LBG showed a broad absorption peak at 3250 cm^{-1} (stretching of -OH group), 2952 cm^{-1} (stretching of –CH), 1748 cm^{-1} (stretching of C=O), and 1000–1100 cm^{-1} (stretching of C-O-H). Upadhyay et al. [41] and Chakravorty et al. [42] found the FTIR spectrum data similar. The FTIR spectrum of pure RE showed a peak at 3330 cm^{-1} (stretching of -OH group), 1730 cm^{-1} (stretching of C=O), and 1120 cm^{-1} (stretching of C-O-H). As we have seen from the FTIR results, we have demonstrated that the apparent OH peak of LBG disappeared and that the rosin glycerol ester is coated with surrounding PEGylated LBG.

3.3 STEM analysis

According to the STEM image of PEG-LBG/RE PNPs (160.000x and 300.000x), we can see that the interior structure of the polymeric nanoparticle is LBG with the size lower than 50 nm. We are able to tell that these particles are small agglomerates of it (**Figure 9**).
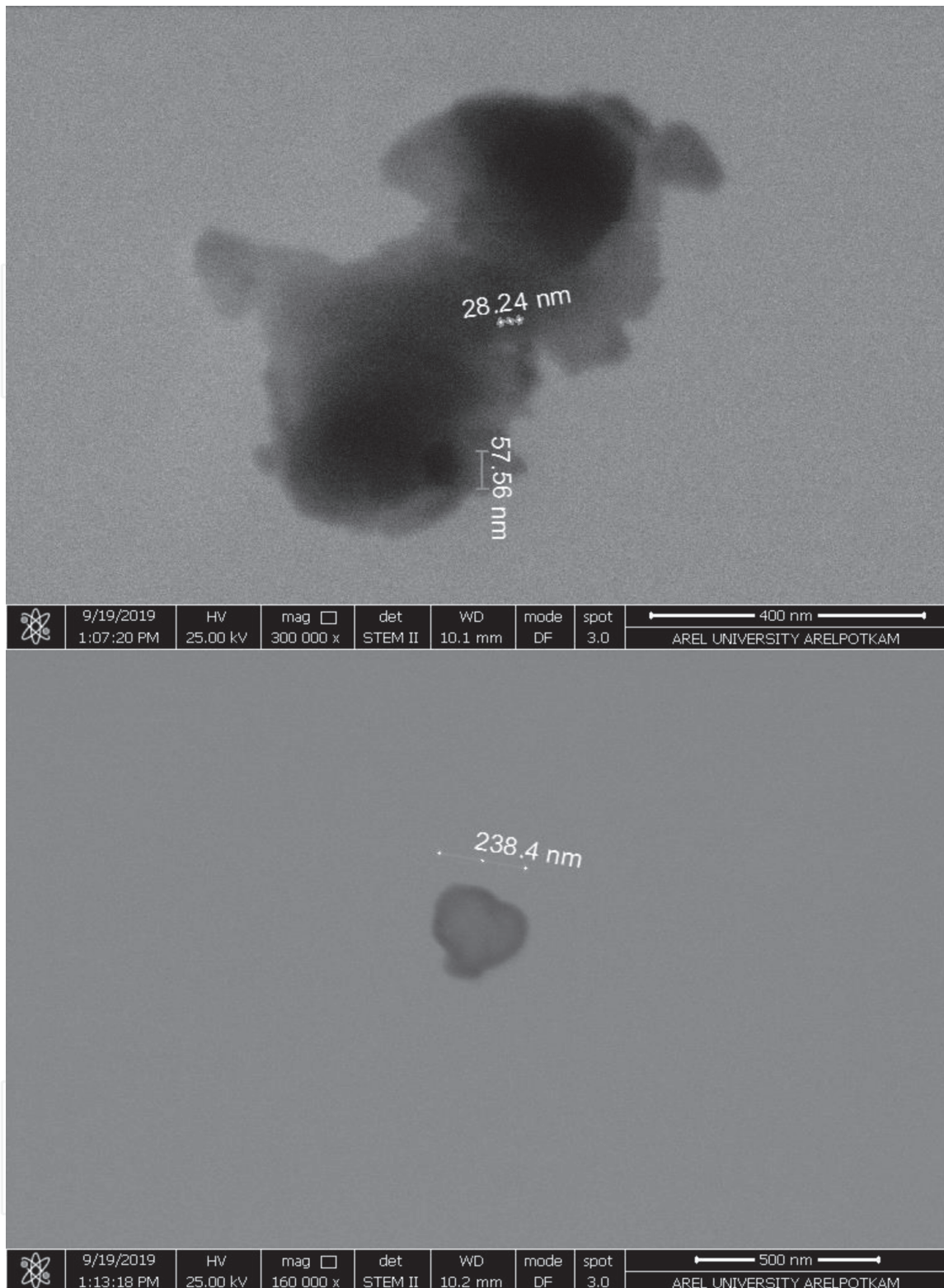
Figure 9.
STEM image of PEG-LBG/RE PNPs (160.000x and 300.000x).

4. Conclusions

We prepared the novel PEG-LBG/RE PNPs with an average particle size of 100 nm using the ultrasonic irradiation. We dispersed the amphiphilic RE coated with PEG-LBG blends in nanosize and spherical structure. We focused on the miscibility of the blends, and shapes of the polymeric nanoparticles were calculated using the values of the intrinsic viscosity in different conditions. We estimate that

PEG-LBG/RE PNPs can be used to increase the therapeutic efficacy and biocompatibility of the nanodrug in pharmaceutical and biomedical studies.

Acknowledgements

Author details

Selcan Karakus[1*], Merve Ilgar[1], Ezgi Tan[1], Yeşim Müge Sahin[2,3], Nevin Tasaltin[4] and Ayben Kilislioglu[1]

1 Department of Chemistry, Faculty of Engineering, Istanbul University-Cerrahpasa, Istanbul, Turkey

2 ArelPOTKAM, Polymer Technologies and Composite Application and Research Center, Istanbul Arel University, Istanbul, Turkey

3 Department of Biomedical Engineering, Faculty of Engineering and Architecture, Istanbul Arel University, Istanbul, Turkey

4 Department of Electrical-Electronics Engineering, Maltepe University, Istanbul, Turkey

*Address all correspondence to: selcan@istanbul.edu.tr

IntechOpen

References

[1] Montasser I, Fessi H, Coleman AW. Atomic force microscopy imaging of novel type of polymeric colloidal nanostructures. European Journal of Pharmaceutics and Biopharmaceutics. 2002;**54**(3):281-284

[2] Bourgeat-Lami E. Organic–inorganic nanostructured colloids. Journal of Nanoscience and Nanotechnology. 2002;**2**(1):1-24

[3] Petry R, Saboia VM, Franqui LS, Holanda CA, Garcia TR, de Farias G, et al. On the formation of protein corona on colloidal nanoparticles stabilized by depletant polymers. Materials Science and Engineering: C.18. 2019;**105**:1-12

[4] Behnajady MA, Eskandarloo H, Modirshahla N, Shokri M. Sol-gel low temperature synthesis of stable anatase type TiO_2 nanoparticles under different conditions and its photocatalytic activity. Photochemistry and Photobiology. 2011;**87**(5):1002-1008

[5] Henglein A. Colloidal silver nanoparticles: Photochemical preparation and interaction with O_2, CCl_4, and some metal ions. Chemistry of Materials. 1998;**10**(1):444-450

[6] Cabrera L, Gutierrez S, Menendez N, Morales MP, Herrasti P. Magnetite nanoparticles: Electrochemical synthesis and characterization. Electrochimica Acta. 2008;**53**(8):3436-3441

[7] Im HJ, Jung EC. Colloidal nanoparticles produced from Cu metal in water by laser ablation and their agglomeration. Radiation Physics and Chemistry. 2016;**118**:6-10

[8] Gasaymeh SS, Radiman S, Heng LY, Saion E, Saeed GM. Synthesis and characterization of silver/polyvinilpirrolidone (Ag/PVP) nanoparticles using gamma irradiation techniques. The African Review of Physics. 2010;**4**:31-41

[9] Tan E, Karakus S, Soylu GSP, Birer Ö, Zengin Y, Kilislioglu A. Formation and distribution of ZnO nanoparticles and its effect on E. coli in the presence of sepiolite and silica within the chitosan matrix via sonochemistry. Ultrasonics Sonochemistry. 2017;**38**:720-725

[10] Gong C, Hart DP. Ultrasound induced cavitation and sonochemical yields. The Journal of the Acoustical Society of America. 1998;**104**(5):2675-2682

[11] Cui D, Mebel AM, Arroyo-Mora LE, Holness H, Furton KG, O'Shea K. Kinetic, product, and computational studies of the ultrasonic induced degradation of 4-methylcyclohexanemethanol (MCHM). Water Research. 2017;**126**:164-171

[12] Masoudian N, Rajabi M, Ghaedi M. Titanium oxide nanoparticles loaded onto activated carbon prepared from bio-waste watermelon rind for the efficient ultrasonic-assisted adsorption of Congo red and phenol red dyes from wastewaters. Polyhedron. 2019;**173**:1-9

[13] Karakuş S. Preparation and rheological characterization of Chitosan-Gelatine@ ZnO-Si nanoparticles. International Journal of Biological Macromolecules. 2019;**137**:821-828

[14] Boufi S, Haaj SB, Magnin A, Pignon F, Impéror-Clerc M, Mortha G. Ultrasonic assisted production of starch nanoparticles: Structural characterization and mechanism of disintegration. Ultrasonics Sonochemistry. 2018;**41**:327-336

[15] Sabaghi V, Davar F, Taherian MH. Ultrasonic-assisted preparation of AlON from alumina/carbon core-shell nanoparticle. Ceramics International. 2019;**45**(3):3350-3358

[16] Dave V, Tak K, Sohgaura A, Gupta A, Sadhu V, Reddy KR. Lipid-polymer hybrid nanoparticles: Synthesis strategies and biomedical applications. Journal of Microbiological Methods. 2019;**160**:130-142

[17] Karakus S, Ilgar M, Kahyaoglu IM, Kilislioglu A. Influence of ultrasound irradiation on the intrinsic viscosity of guar gum–PEG/rosin glycerol ester nanoparticles. International Journal of Biological Macromolecules. 2019;**141**: 1118-1127

[18] Barak S, Mudgil D. Locust bean gum: Processing, properties and food applications—A review. International Journal of Biological Macromolecules. 2014;**66**:74-80

[19] Jayapal JJ, Dhanaraj S. Exemestane loaded alginate nanoparticles for cancer treatment: Formulation and in vitro evaluation. International Journal of Biological Macromolecules. 2017;**105**: 416-421

[20] Yu S, Xu X, Feng J, Liu M, Hu K. Chitosan and chitosan coating nanoparticles for the treatment of brain disease. International Journal of Pharmaceutics. 2019;**560**:282-293

[21] Sethi S, Kaith BS, Kumar V. Fabrication and characterization of microwave assisted carboxymethyl cellulose-gelatin silver nanoparticles imbibed hydrogel: Its evaluation as dye degradation. Reactive and Functional Polymers. 2019;**142**:134-146

[22] Şişmanoğlu T, Karakuş S, Birer Ö, Soylu GSP, Kolan A, Tan E, et al. Preparation and characterization of antibacterial Senegalia (Acacia) Senegal/iron–silica bio-nanocomposites. Applied Surface Science. 2015;**354**: 250-255

[23] Patra AS, Ghorai S, Ghosh S, Mandal B, Pal S. Selective removal of toxic anionic dyes using a novel nanocomposite derived from cationically modified guar gum and silica nanoparticles. Journal of Hazardous Materials. 2016;**301**:127-136

[24] Pooja D, Panyaram S, Kulhari H, Rachamalla SS, Sistla R. Xanthan gum stabilized gold nanoparticles: Characterization, biocompatibility, stability and cytotoxicity. Carbohydrate Polymers. 2014;**110**:1-9

[25] Braz L, Grenha A, Ferreira D, da Costa AMR, Gamazo C, Sarmento B. Chitosan/sulfated locust bean gum nanoparticles: In vitro and in vivo evaluation towards an application in oral immunization. International Journal of Biological Macromolecules. 2017;**96**:786-797

[26] Pawar HA, Lalitha KG, Ruckmani K. Alginate beads of captopril using galactomannan containing Senna tora gum, guar gum and locust bean gum. International Journal of Biological Macromolecules. 2015;**76**:119-131

[27] Perestrelo AR, Grenha A, da Costa AMR, Belo JA. Locust bean gum as an alternative polymeric coating for embryonic stem cell culture. Materials Science and Engineering: C. 2014;**40**: 336-344

[28] Higiro J, Herald TJ, Alavi S, Bean S. Rheological study of xanthan and locust bean gum interaction in dilute solution: Effect of salt. Food Research International. 2007;**40**(4):435-447

[29] Cordeiro T, Paninho AB, Bernardo M, Matos I, Pereira CV, Serra AT, et al. Biocompatible locust bean gum as mesoporous carriers for naproxen delivery. Materials Chemistry and Physics. 2020;**239**:121973

[30] Braz L, Grenha A, Corvo MC, Lourenco JP, Ferreira D, Sarmento B, et al. Synthesis and characterization of locust bean gum derivatives and their

application in the production of nanoparticles. Carbohydrate Polymers. 2018;**181**:974-985

[31] Soumya RS, Sherin S, Raghu KG, Abraham A. Allicin functionalized locust bean gum nanoparticles for improved therapeutic efficacy: An in silico, in vitro and in vivo approach. International Journal of Biological Macromolecules. 2018;**109**:740-747

[32] Behrouzian F, Razavi SM, Karazhiyan H. Intrinsic viscosity of cress (*Lepidium sativum*) seed gum: Effect of salts and sugars. Food Hydrocolloids. 2014;**35**:100-105

[33] Huggins ML. The viscosity of dilute solutions of long-chain molecules. IV. Dependence on concentration. Journal of the American Chemical Society. 1942;**64**(11):2716-2718

[34] Kraemer EO. Molecular weights of cellulose and cellulose derivatives. Industrial & Engineering Chemistry. 1938;**30**(10):1200-1203

[35] Tanglertpaibul T, Rao MA. Intrinsic viscosity of tomato serum as affected by methods of determination and methods of processing concentrates. Journal of Food Science. 1987;**52**(6):1642-1645

[36] Chen HH, Kang HY, Chen SD. The effects of ingredients and water content on the rheological properties of batters and physical properties of crusts in fried foods. Journal of Food Engineering. 2008;**88**(1):45-54

[37] Razavi SM, Moghaddam TM, Emadzadeh B, Salehi F. Dilute solution properties of wild sage (*Salvia macrosiphon*) seed gum. Food Hydrocolloids. 2012;**29**(1):205-210

[38] Jiang WH, Han SJ. The interactions of chitosan–poly (ethylene glycol) in the presence of added salt in water: Viscosity effect. European Polymer Journal. 1999;**35**(11):2079-2085

[39] Li F, Li L, Zhong G, Zhai Y, Li Z. Effects of ultrasonic time, size of aggregates and temperature on the stability and viscosity of Cu-ethylene glycol (EG) nanofluids. International Journal of Heat and Mass Transfer. 2019;**129**:278-286

[40] Curvale R, Masuelli M, Padilla AP. Intrinsic viscosity of bovine serum albumin conformers. International Journal of Biological Macromolecules. 2008;**42**(2):133-137

[41] Upadhyay M, Adena SKR, Vardhan H, Yadav SK, Mishra B. Locust bean gum and sodium alginate based interpenetrating polymeric network microbeads encapsulating Capecitabine: Improved pharmacokinetics, cytotoxicity &in vivo antitumor activity. Materials Science and Engineering: C. 2019;**104**:109958

[42] Chakravorty A, Barman G, Mukherjee S, Sa B. Effect of carboxymethylation on rheological and drug release characteristics of locust bean gum matrix tablets. Carbohydrate Polymers. 2016;**144**:50-58